blood®
Regular Article

IMMUNOBIOLOGY AND IMMUNOTHERAPY

# INPP5K controls the dynamic structure and signaling of wild-type and mutated, leukemia-associated IL-7 receptors

Bastien Moës,[1] Hua Li,[2] Patricia Molina-Ortiz,[1] Coraline Radermecker,[3] Adeline Rosu,[4] Charles-Andrew Vande Catsyne,[1] Sufyan Ali Sayyed,[1] João Fontela,[5] Mafalda Duque,[5] Alice Mostafa,[1] Abdelhalim Azzi,[1] João T. Barata,[5] Ramon Merino,[6] Chenqi Xu,[2,7] Christophe J. Desmet,[4] and Stéphane Schurmans[1]

[1]Laboratory of Functional Genetics, GIGA Research Centre, Université de Liège, Liège, Belgium; [2]State Key Laboratory of Molecular Biology, Shanghai Institute of Biochemistry and Cell Biology, Center for Excellence in Molecular Cell Science, Chinese Academy of Sciences, University of Chinese Academy of Sciences, Shanghai, China; [3]Laboratory of Immunophysiology and [4]Laboratory of Cellular and Molecular Immunology, GIGA Research Centre, Université de Liège, Liège, Belgium; [5]Instituto de Medicina Molecular João Lobo Antunes, Faculdade de Medicina da Universidade de Lisboa, Lisbon, Portugal; [6]Instituto de Biomedicina y Biotecnología de Cantabria, CSIC-Universidad de Cantabria-SODERCAN, Santander, Spain; and [7]School of Life Science, Hangzhou Institute for Advanced Study, University of Chinese Academy of Sciences, Hangzhou, China

KEY POINTS

- **We identified a role and the mechanism of action of INPP5K in the control of the dynamic structure and signaling of the wild-type IL-7R.**
- **Silencing INPP5K in a cell line expressing a mutant human IL-7Rα chain that triggers leukemia resulted in reduced cell proliferation.**

**The downstream signaling of the interleukin-7 (IL-7) receptor (IL-7R) plays important physiological and pathological roles, including the differentiation of lymphoid cells and proliferation of acute lymphoblastic leukemia cells. Gain-of-function mutations in the IL-7Rα chain, the specific component of the receptor for IL-7, result in constitutive, IL-7–independent signaling and trigger acute lymphoblastic leukemia. Here, we show that the loss of the phosphoinositide 5-phosphatase INPP5K is associated with increased levels of the INPP5K substrate phosphatidylinositol 4,5-bisphosphate (PtdIns[4,5]P2) and causes an altered dynamic structure of the IL-7 receptor. We discovered that the IL-7Rα chain contains a very conserved positively charged polybasic amino acid sequence in its cytoplasmic juxtamembrane region; this region establish stronger ionic interactions with negatively charged PtdIns(4,5)P2 in the absence of INPP5K, freezing the IL-7Rα chain structure. This dynamic structural alteration causes defects in IL-7R signaling, culminating in decreased expressions of EBF1 and PAX5 transcription factors, in microdomain formation, cytoskeletal reorganization, and bone marrow B-cell differentiation. Similar alterations after the reduced INPP5K expression also affected mutated, constitutively activated IL-7Rα chains that trigger leukemia development, leading to reduced cell proliferation. Altogether, our results indicate that the lipid 5-phosphatase INPP5K hydrolyzes PtdIns(4,5)P2, allowing the requisite conformational changes of the IL-7Rα chain for optimal signaling.**

## Introduction

The interleukin-7 (IL-7) receptor (IL-7R) is formed by a heterodimer of IL-7Rα (CD127) and the common γ chain (γc; CD132) (reviewed by Palmer et al[1]). The binding of IL-7 to its receptor induces conformational changes in IL-7Rα and γc ectodomains, pulling their cytoplasmic domains closer together. As a consequence, IL-7Rα and γc cytoplasmic domain-bound JAK1 and JAK3 transphosphorylate each other and activate STAT proteins.[2-4] Phosphorylated STAT proteins translocate into the nucleus and activate transcription of prosurvival and proliferation proteins.

IL-7R signaling is essential for the normal development and maintenance of the entire lymphoid compartment, but the importance of keeping IL-7R signaling under control is illustrated with studies showing that IL-7 transgenic mice develop B-cell lymphomas, and IL-7 stimulates the proliferation of human acute lymphoblastic leukemia (ALL) cells. These findings, and others, indicate that signaling downstream of the wild-type IL-7R contributes to leukemia development (reviewed by Barata et al[5]). In addition, somatic gain-of-function mutations in the IL-7Rα chain were identified in T- and B-ALL cases. ALL-associated mutations in the IL-7Rα chain lead to constitutive, IL-7–independent signaling and trigger leukemia.[6-8]

Inositol polyphosphate 5-phosphatase K (INPP5K) is a member of the phosphoinositide (PI) 5-phosphatases family whose protein structure is composed of an N-terminal catalytic domain that hydrolyzes both phosphatidylinositol 4,5-bisphosphate

(PtdIns[4,5]P2) and phosphatidylinositol 3,4,5-trisphosphate (PtdIns[3,4,5]P3), followed by a SKIP carboxyl homology (SKICH) domain at the C-terminus, responsible for protein-protein interactions and the subcellular localization of the enzyme (reviewed by Schurmans et al[9]). We previously reported that the *Inpp5k* messenger RNA is abundantly expressed in the mouse hematopoietic system, including in B cells.[10] However, the role of this PI 5-phosphatase in B cells is totally unknown. Thus, the general objective of this study was to define the functions and mechanisms of action of INPP5K in B cells using a new genetically modified mouse model that allowed cell-specific inactivation of this 5-phosphatase.

# Materials and methods

## Statistical analysis

Assumptions of normal distribution of residuals and homoscedasticity were verified, and data were presented as the mean + standard error of the mean as well as individual values, unless otherwise indicated. Data from independent experiments were pooled for analysis in each data panel, unless otherwise indicated. Statistical analyses were performed using Prism 8 (GraphPad). Unpaired *t* test was performed, unless otherwise indicated in the figure legends. We considered a *P* value lower than .05 as significant. Nonsignificant P values: $P > .05$; *$P < .05$; **$P < .01$; ***$P < .001$; ****$P < .0001$.

Complete information about materials and methods is presented in supplemental Material 1, available on the *Blood* website.

# Results

## Loss of INPP5K alters IL-7R signaling and Pax5 expression in fractions A and B of developing B cells

A conditional knockout *Inpp5k*$^{flox/flox}$ Vav-Cre (VAV-CRE) mouse model was generated to study the effects of *Inpp5k* gene inactivation on hematopoiesis (supplemental Material 2). In the blood of these VAV-CRE mice, the total leukocyte, lymphocyte, CD19$^+$ B-cell, and immunoglobulin concentrations were significantly decreased, as compared with those of control mice. Alterations in B-cell differentiation and maturation were identified at critical stages known to be controlled by the IL-7R/PAX5 signaling pathway and by the cell-surface expression of the pre–B-cell receptor and the B-cell receptor (supplemental Material 2).

In mice, the IL-7R/PAX5 signaling pathway plays an essential role in initiating and maintaining B-cell lineage commitment in the bone marrow. Cell-surface expressions of IL-7Rα and γc were similar in fractions A and B of VAV-CRE and control mice (supplemental Figure 9A). By contrast, PAX5 protein expression was significantly decreased in these 2 fractions in VAV-CRE mice as compared with those in control mice (Figure 1A), leading to rearrangement defects at the immunoglobulin heavy chain locus (supplemental Material 3). Because the level of PAX5 during early bone marrow B-cell differentiation is controlled by PI3K/PtdIns(3,4,5)P3/AKT and JAK1-3/STAT5/EBF1 signaling downstream to the IL-7R,[11-15] the activities of these signaling pathways were compared in VAV-CRE and control bone marrow B cells. Levels of phospho-AKT (p-AKT) and total AKT were similar in VAV-CRE and control B cells from fractions A and B, both before and 2 to 10 minutes after the addition of IL-7 (Figure 1B; supplemental Figure 9A). Because p-AKT was proposed to negatively control PAX5 levels in bone marrow B cells,[14] our results suggest that the PI3K/PtdIns(3,4,5)P3/AKT signaling is responsible neither for the decreased level of PAX5 nor the partial blockade observed between fractions A and B during VAV-CRE B-cell differentiation. In contrast with this, levels of EBF1, a transcription factor that is connected to PAX5 in a complex positive feedback loop,[12,13,15-17] were significantly decreased in VAV-CRE B cells from fractions A and B as compared with those in control B cells (Figure 1C). Upstream of EBF1, the p-STAT5 levels were also significantly decreased in VAV-CRE B cells from fractions A and B as compared with those in control B cells, both before and up to 10 minutes after the addition of IL-7, despite similar or slightly increased levels of total STAT5 (Figure 1D; supplemental Figure 9A). Upstream of STAT5, in B cells from fraction A, levels of p-JAK1 and p-JAK3 were significantly decreased in VAV-CRE mice compared with those in control mice, both before and up to 10 minutes after the addition of IL-7, despite similar levels of total JAK1 and JAK3 (Figure 1E-F; supplemental Figure 9A). Data were slightly more complex in the few B cells remaining in fraction B of VAV-CRE mice: levels of p-JAK1 in this fraction were also significantly decreased, as in fraction A, but p-JAK3 levels tended to be slightly increased in VAV-CRE B cells from fraction B, as compared with the levels in control B cells (Figure 1E-F). Again, total JAK1 and JAK3 levels were similar in VAV-CRE and control B cells from fraction B, as in those from fraction A (supplemental Figure 9A). Finally, levels of p–IL-7Rα$^{Y449}$, the phospho-tyrosine that seems essential for the binding of STAT5 and regulatory subunits of class IA PI3K to the carboxy-terminal end of the IL-7Rα cytoplasmic domain,[18-22] were not significantly different in the cells of fractions A and B in control and VAV-CRE mice (supplemental Figure 9B). It is noteworthy here that PAX5 and EBF1 levels were also significantly decreased in B cells from fraction B in *Inpp5k*$^{flox/flox}$ MB1-Cre mice, in which *Inpp5k* is specifically inactivated in the B-cell lineage (supplemental Figure 11). Altogether, our results indicate that the loss of INPP5K expression in bone marrow B cells negatively affects the early steps of IL-7R signaling in these cells.

## Loss of INPP5K alters IL-7R and IL-7R–bound JAK kinase dynamic structure

The conformational changes in IL-7R induced by IL-7 binding were analyzed using an indirect fluorescence resonance energy transfer (FRET) assay described by Guala et al.[23] To validate this assay in control bone marrow B220$^+$CD43$^+$ B cells, we first defined the maximal and the minimal FRET efficiency using donor and acceptor fluorophore-labeled antibodies directed either against the same target (JAK1; close proximity; positive control) or against 2 targets present in different subcellular compartments (JAK1 in the cytoplasm and PAX5 in the nucleus; remoteness; negative control). As expected, the energy transfer between the excited donor and acceptor fluorophores, or FRET efficiency, was high when antibodies bound to the same JAK1 target and close to zero when they bound to JAK1 and PAX5 remote targets (supplemental Figure 12). Secondly, we tested whether this indirect FRET assay was able to detect the

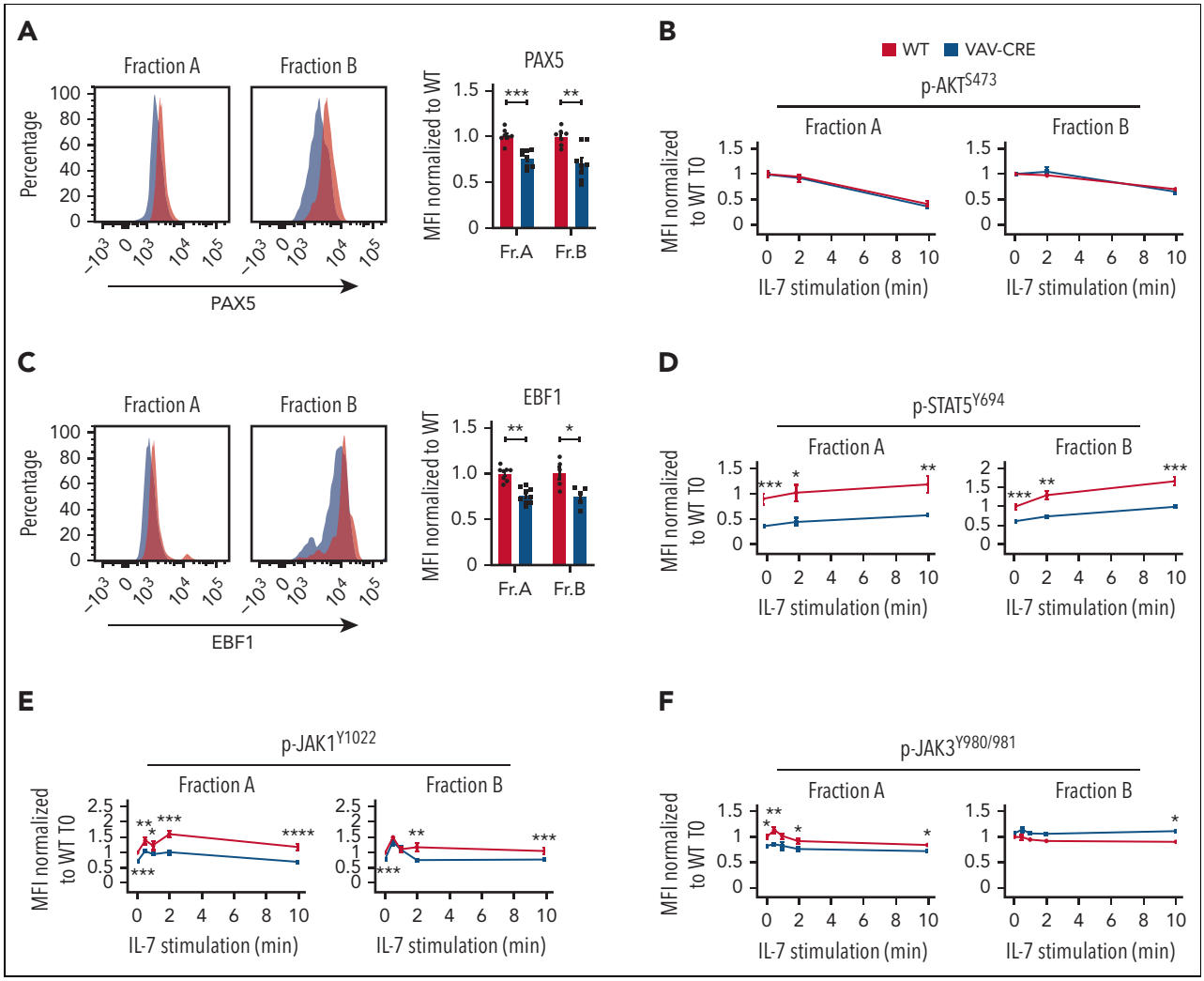


**Figure 1. *Inpp5k* inactivation results in altered IL-7R signaling and Pax5 expression in fractions A and B of the bone marrow.** (A) PAX5 protein expression was analyzed using flow cytometry after plasma and nuclear membrane permeabilization of control (WT, red areas and columns) and VAV-CRE (blue areas and columns) cells from fractions A and B. Representative MFI histograms of PAX5 protein expression (left). Quantified expression of PAX5 protein after MFI normalization to WT with mean MFI (right). Results represent individual mice (n = 8-9 mice per group) and mean ± SEM. (B) Flow cytometry analysis of p-AKT$^{S473}$ in plasma membrane–permeabilized cells from fractions A and B isolated from control (WT, red lines) and VAV-CRE (blue lines) mice, before (0) and 2 to 10 minutes after ex vivo addition of IL-7 (2 ng/mL) at 37°C. Quantitative expression of p-AKT$^{S473}$ normalized to WT with mean MFI at t = 0 (before IL-7 addition). Results are representative of 2 independent experiments for a total of 6 mice. (C) EBF1 protein expression was analyzed using flow cytometry after plasma and nuclear membrane permeabilization of control (WT, red areas and columns) and VAV-CRE (blue areas and columns) cells from fractions A and B. Representative MFI histograms of EBF1 protein expression (top). The quantitative expression of EBF1 protein after MFI normalization to WT with mean MFI (bottom). Results represent individual mice (n = 5-9 mice per group) and mean ± SEM. (D) Flow cytometry analysis of p-STAT5$^{Y694}$ in plasma membrane–permeabilized cells from fractions A and B isolated from control (WT, red lines) and VAV-CRE (blue lines) mice, before (0) and 2 to 10 minutes after the ex vivo addition of IL-7 (2 ng/mL) at 37°C. Quantitative expression of p-STAT5$^{Y694}$ normalized to WT with mean MFI at t = 0 (before IL-7 addition). Results are representative of a total of 6 mice. (E-F) Flow cytometry analysis of p-JAK1$^{Y1022}$ (E) and p-JAK3$^{Y980/981}$ (F) in plasma membrane–permeabilized cells from fractions A and B isolated from control (WT, red lines) and VAV-CRE (blue lines) mice, before (0), 0.5, 1, 2, and 10 minutes after the ex vivo addition of IL-7 (2 ng/mL) at 37°C. Quantified expression of p-JAK1$^{Y1022}$ (E) and p-JAK3$^{Y980/981}$ (F) normalized to WT MFI at t = 0 (before IL-7 addition). Results are representative of 4 independent experiments for a total of 8 to 12 mice. *P* values were calculated using unpaired nonparametric *t* test. NS: $P > .05$; *$P < .05$; **$P < .01$; ***$P < .001$; ****$P < .0001$. NS, nonsignificant; MFI, mean fluorescence intensity; SEM, standard error of the mean; WT, wild type.

structural changes in IL-7R, as reported in the literature regarding the response to IL-7. For this purpose, the relative proximity between IL-7Rα and γc ectodomains and between JAK1 and JAK3 was analyzed in control bone marrow B220$^+$CD43$^+$ B cells in response to IL-7 (Figure 2A-C). The energy transfer between the excited donor and the acceptor fluorophore-labeled antibodies bound either to γc and IL-7Rα ectodomains or to JAK3 and JAK1 significantly increased after the addition of IL-7, reflecting their closer proximity in activated IL-7R, in agreement with previous reports (Figure 2B-C). By contrast, the analysis of B220$^+$CD43$^+$ VAV-CRE bone marrow B cells revealed a different pattern of energy transfer between the same targets, despite their similar expression in control and VAV-CRE B cells (Figure 2B-C; supplemental Figure 9). Indeed, in VAV-CRE B cells, energy transfer between excited donor and acceptor fluorophore-labeled antibodies bound to γc and IL-7Rα ectodomains was significantly lower than that in control B cells, both in basal and IL-7–stimulated conditions, suggesting that the 2 ectodomains of the IL-7R are more distant when *Inpp5k* is inactivated (Figure 2B). Moreover, the energy transfer between the excited donor and acceptor fluorophore-labeled antibodies bound to JAK3 and JAK1 in the basal condition

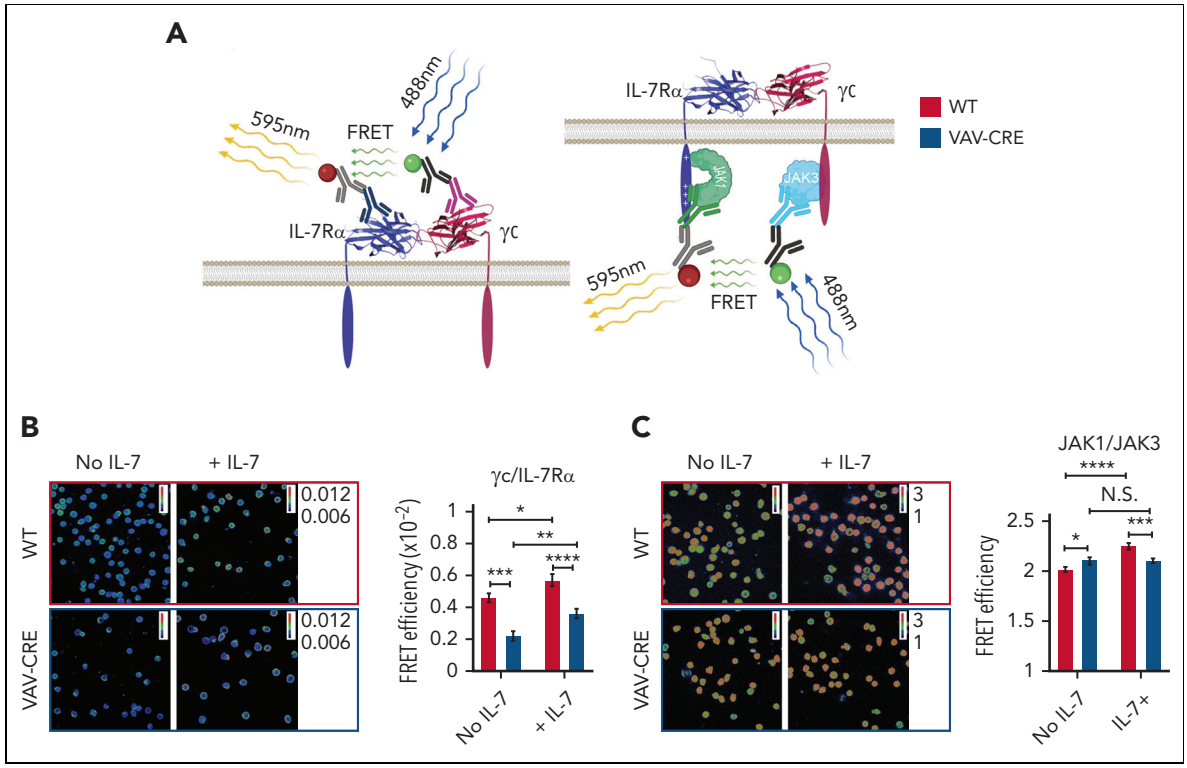


**Figure 2. *Inpp5k* inactivation alters IL-7R and IL-7R–bound JAK kinases dynamic structure.** (A) An indirect FRET strategy was used to analyze the proximity between IL-7Rα and γc ectodomains (left) and between JAK1 and JAK3 (right). Primary antibodies directed against IL-7Rα and γc ectodomains or against JAK1 and JAK3 as well as fluorophore-labeled secondary antibodies that specifically recognized the constant part of one of the primary antibodies were used. The green marker attached to the first secondary antibody represents the donor fluorophore (AF488), and the red one attached to the other secondary antibody represents the acceptor fluorophore (AF546). The closer the distance between the 2 probed proteins (IL-7Rα and γc ectodomains; JAK1 and JAK3), the higher the energy transfer and the resulting FRET signal (FRET efficiency). (B-C) Indirect FRET analysis of IL-7Rα/γc ectodomains (B) and JAK1/JAK3 (C) proximity in sorted $B220^+CD43^+$ bone marrow cells from control (WT, red columns) and VAV-CRE (blue columns) mice, before and after addition of IL-7 (2 ng/mL) for 2 minutes at 37°C. (B) Representative confocal pictures (original magnification ×63) of energy transfer (FRET efficiency) between AF488 (γc) and AF546 (IL-7Rα) labeled secondary antibodies. FRET efficiency was calculated in accordance with the indirect FRET method validated by Guala et al (left).[23] The rainbow scale represents the energy transfer between the 2 fluorophores, from 0.006 (blue) to 0.012 (white). The quantitative energy transfer between the 2 indirectly labeled γc and IL-7Rα ectodomains (FRET efficiency) is presented (right). Results represent mean ± SEM (n = 148-220 cells analyzed per group, from 6 mice). (C) Representative confocal pictures (original magnification ×63) of energy transfer (FRET efficiency) between AF488 (JAK3)- and AF546 (JAK1)-labeled secondary antibodies (left). FRET efficiency was calculated as described earlier. The rainbow scale represents the energy transfer between the 2 fluorophores, from 1 (blue) to 3 (white). The quantitative energy transfer between indirectly labeled JAK3 and JAK1 (FRET efficiency) is presented (right). Results represent mean ± SEM (n = 180-242 cells analyzed per group, from 6 mice). *P* values were calculated using unpaired nonparametric *t* test. NS: $P > .5$; $^*P < .5$; $^{**}P < .1$; $^{***}P < .01$; $^{****}P < .001$. NS, nonsignificant; SEM, standard error of the mean; WT, wild type; FRET, fluorescence resonance energy transfer.

was slightly but significantly higher in VAV-CRE B cells than in control B cells, suggesting a closer proximity between these kinases in the absence of INPP5K and IL-7 (Figure 2C). Surprisingly, the addition of IL-7 did not modify the energy transfer between JAK3 and JAK1 in VAV-CRE B cells, and this energy transfer was significantly lower than that in control B cells (Figure 2C). Altogether, our indirect FRET results indicate that significant alterations occur in the conformational structure of the IL-7R when *Inpp5k* is inactivated, both in basal conditions and after the addition of IL-7. Importantly, they also indicate that the distance between the IL-7R cytoplasmic domain-bound JAK1 and JAK3 is reduced in basal conditions in VAV-CRE B cells compared with that in control B cells but unchanged in response to IL-7. In other words, the IL-7R in VAV-CRE B cells appears frozen in a state intermediate between basal and IL-7–stimulated conditions in control B cells.

## Role of PtdIns(4,5)P2 and the IL-7Rα cytoplasmic domain in the control of IL-7R dynamic structure

INPP5K comprises an N-terminal catalytic domain that hydrolyzes both PtdIns(4,5)P2 and PtdIns(3,4,5)P3 substrates.[9] As mentioned earlier, levels of p-AKT and total AKT before and after IL-7 stimulation were similar in VAV-CRE and control B cells of fractions A and B. This suggests that PtdIns(3,4,5)P3 does not play a major role in the phenotype of VAV-CRE bone marrow B cells. In contrast, flow cytometry analysis revealed that the PtdIns(4,5)P2 signal was significantly increased in VAV-CRE B cells of fractions A and B, as compared with that in control B cells (Figure 3A, left and middle panels). Immunofluorescence studies on $B220^+CD43^+$ bone marrow B cells confirmed that the PtdIns(4,5)P2 signal had increased in VAV-CRE mice compared with that in control mice (Figure 3A, right panel). There are multiple functional roles assigned to PtdIns(4,5)P2. Notably, ionic interactions between its negatively charged phosphates and polybasic amino acid sequences present in membrane proteins, including receptors, are known to regulate protein structure and function (reviewed by Li et al[24]). These positively charged polybasic amino acid sequences are classically localized in the cytoplasmic domain of the protein, close to the transmembrane domain, allowing interaction with acidic phospholipids present in the inner leaflet of the plasma membrane. These sequences are organized in

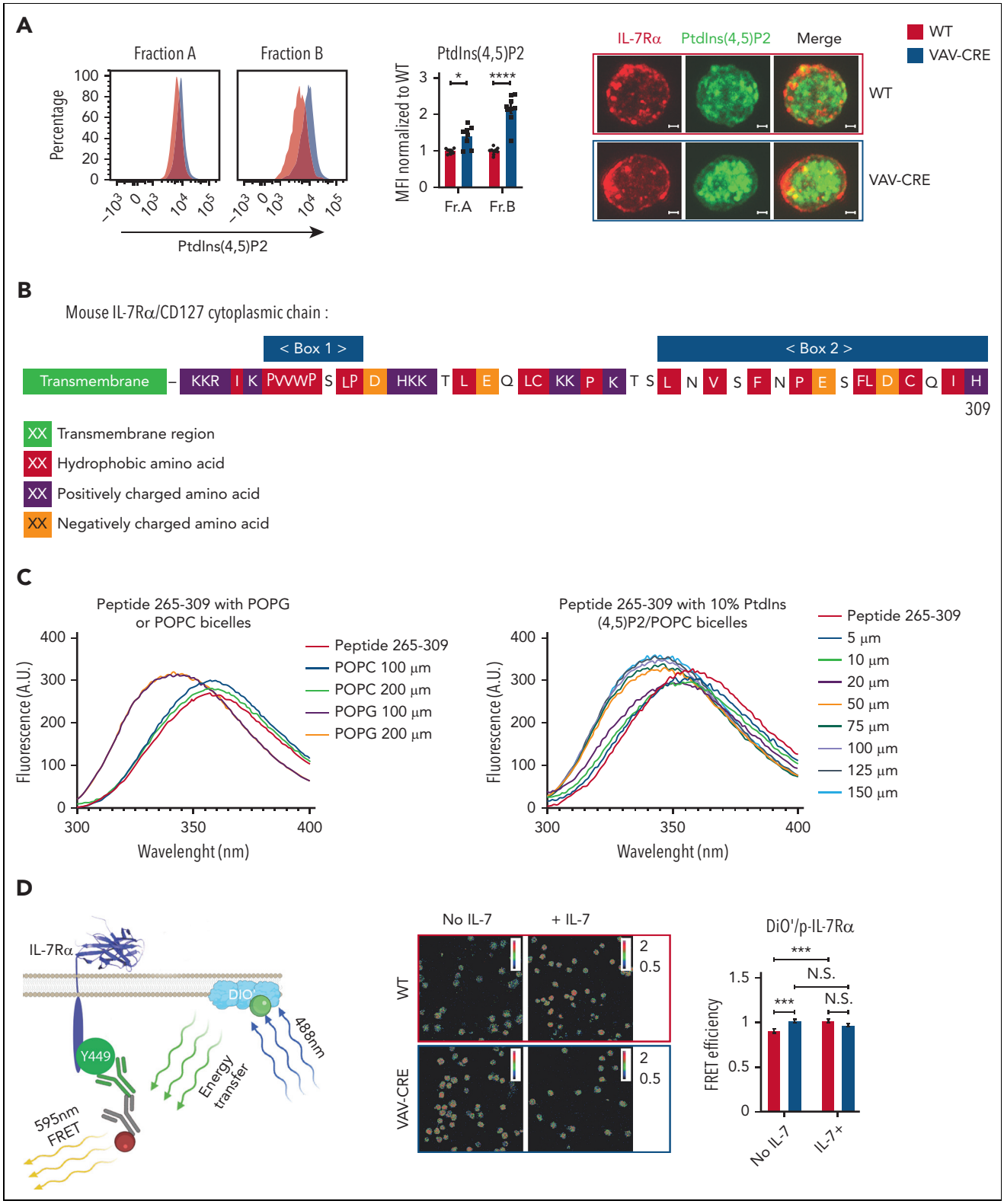


**Figure 3. Role of PtdIns(4,5)P2 and the IL-7Rα cytoplasmic domain in the control of IL-7R dynamic structure.** (A) The PtdIns(4,5)P2 signal was analyzed using flow cytometry and confocal microscopy in plasma membrane–permeabilized cells from fractions A and B (for flow cytometry) and in plasma membrane–permeabilized sorted bone marrow B220$^{+}$CD43$^{+}$ cells (for confocal microscopy) from control (WT, red areas and columns) and VAV-CRE (blue areas and columns) mice. Representative MFI histograms of PtdIns(4,5)P2 signal (left). Quantitative PtdIns(4,5)P2 signal after MFI normalization to WT with mean MFI (middle). Results represent individual mice (n = 9 mice per group) and means ± SEM. Representative confocal microscopy pictures (original magnification ×100) of bone marrow B220$^{+}$CD43$^{+}$ sorted cells from WT and VAV-CRE mice. The IL-7Rα (red) antibody was added to cells before plasma membrane–permeabilization, whereas the PtdIns(4,5)P2 (green) antibody was added after membrane permeabilization. White scale bars: 1 µm. (B) The positively charged polybasic 45 amino acid sequence in the juxtamembrane region of the mouse IL-7Rα cytoplasmic domain is presented. Box 1 and 2 (blue) represent the 2 JAK1 binding domains on the IL-7Rα chain. The transmembrane region (green), hydrophobic (red), positively (purple), and

clusters of basic amino acids that are separated by a suitable distance, which is ideal for interaction with PtdIns(4,5)P2 and its multiple charges; these clusters are separated by hydrophobic residues, which further stabilize the ionic protein-lipid interaction, and contain very few acidic residues.[24] Analysis of the amino acid sequence of the γc cytoplasmic domain did not reveal the presence of a polybasic sequence. By contrast, in the IL-7Rα chain, a positively charged polybasic sequence of 45 amino acids was detected that fulfilled all the above criteria to participate in ionic interactions with PtdIns(4,5)P2 (Figure 3B). This sequence in the juxtamembrane region of the IL-7Rα cytoplasmic domain has an isoelectric point of 9.4, meaning a net positive charge of 4.2 at physiological pH (by contrast, the whole 195 amino acid–long IL-7Rα cytoplasmic domain has an isoelectric point of 7.3, meaning a net negative charge of 0.1 at physiological pH). It is also remarkably conserved between species, suggesting an important functional role (supplemental Figure 13). To address the hypothesis that this 45 amino acid sequence interacts with PtdIns(4,5)P2 in the inner leaflet of the plasma membrane, a tryptophan fluorescence emission spectrum assay was used. We used this assay to assess the interaction of a synthesized peptide comprising amino acids 265 to 309 of the IL-7Rα sequence with large bicelles of different lipid compositions (Figure 3C). The tryptophan spectrum of the peptide showed an obvious blue shift in the presence of negatively charged bicelles of acidic 1-palmitoyl-2-oleoyl-sn-glycero-3-phosphatidylglycerol (POPG), but not in the presence of neutral bicelles of zwitterionic 1-palmitoyl-2-oleoyl-sn-glycero-3-phosphatidylcholine (POPC) (Figure 3C, left panel). These results demonstrate that the microenvironment of the tryptophan residue within the peptide specifically changed when interacting with acidic lipid bicelles. When bicelles containing 10% acidic PtdIns(4,5)P2 and 90% neutral POPC were used in the tryptophan fluorescence emission spectrum assay, no significant interaction between the peptide and bicelles was detected at low lipid concentrations (5-20 μM). By contrast, at higher lipid concentrations (50-150 μM), the tryptophan spectrum of the peptide showed a blue shift, demonstrating that the peptide interacts with acidic PtdIns(4,5)P2 only at high lipid/PtdIns(4,5)P2 concentrations (Figure 3C, right panel). A mutational analysis of the 3 clusters of basic amino acids present in the peptide revealed that they are all important to establish ionic interactions with PtdIns(4,5)P2/POPC bicelles (supplemental Figure 14). To analyze the proximity between the IL-7Rα chain cytoplasmic domain and the plasma membrane, a likely reflection of the strength of ionic interactions between the IL-7Rα chain polybasic sequence and plasma membrane PtdIns(4,5)P2, we used a donor fluorophore-labeled DiO′ membrane probe and an acceptor fluorophore-labeled antibody directed against p–IL-7Rα$^{Y449}$ in an indirect FRET assay (Figure 3D). In the basal condition, the energy transfer between the excited donor 3,3′-dioctadecylox-acarbocyanine perchlorate (DiO′) membrane fluorophore and the acceptor fluorophore-labeled antibody bound to p–IL-7Rα$^{Y449}$, which is similarly expressed and phosphorylated in control and VAV-CRE B cells (supplemental Figure 9A-B), was significantly higher in VAV-CRE B cells compared with that in control B cells. This result reflects the closer proximity of p–IL-7Rα$^{Y449}$ to the plasma membrane when *Inpp5k* is inactivated (Figure 3D). The addition of IL-7 to control B cells significantly increased energy transfer between the excited donor DiO′ membrane fluorophore and the acceptor fluorophore-labeled antibody bound to p–IL-7Rα$^{Y449}$ as compared with that in the basal condition. By contrast, energy transfer was not modified after the addition of IL-7 to VAV-CRE *Inpp5k*–deficient B cells (Figure 3D). Altogether, our FRET results indicate that in basal conditions, the distance between the polybasic sequence–containing IL-7Rα cytoplasmic domain and the plasma membrane is lower in B cells with a loss of INPP5K compared with that in control B cells, suggesting an increased ionic interaction between the polybasic sequence and PtdIns(4,5)P2. Moreover, in *Inpp5k*–deficient B cells, this distance is not modified by the addition of IL-7 and seems frozen in a state which is intermediate between basal and IL-7–stimulated conditions in control B cells, likely causing the perturbations observed in IL-7R signaling. Concomitantly with this altered dynamic structure, the binding of IL-7 to its receptor on VAV-CRE B220$^{+}$CD43$^{+}$ bone marrow B cells led to defects in membrane and cytoskeletal reorganization compared with that in control B cells (supplemental Material 4).

## INPP5K knockdown alters the structure and reduces constitutive signaling of mutated ALL-associated human IL-7Rα chains

ALL-associated mutations in the human IL-7Rα chain are somatic, heterozygous, and affect either exon 5 or 6, falling into 4 classes. Type 1a mutations are the most frequent, occur in exon 6, and are insertions or insertion-deletions that include an unpaired cysteine in the extracellular juxtamembrane-transmembrane portion of the IL-7Rα chain. These mutations lead to a disulfide bond–dependent mutant IL-7Rα chain homodimerization and constitutive, IL-7–independent signaling.[5] The possibility that INPP5K knockdown could alter the structure and signaling of mutated, constitutively activated (CA) IL-7Rα chains was tested in mouse BaF3 cells expressing the type 1a human IL-7Rα p.Thr244_Ile245 insCysProThr mutant (hereafter referred to as CA–IL-7Rα). Indeed, this mutant, like all CA–IL-7Rα mutants discovered so far, leaves intact the cytoplasmic polybasic amino acid sequence identified earlier. Five lentiviruses expressing different short hairpin RNAs (shRNAs) directed against the mouse *Inpp5k* messenger RNA were used to transduce the CA–IL-7Rα chain–expressing BaF3 cells. With the most efficient shRNA anti-*Inpp5k*, the residual INPP5K signal was 20% to 25%

**Figure 3 (continued)** negatively (orange) charged amino acids are represented. (C) A tryptophan fluorescence emission spectrum assay was used to detect the binding of the 45 amino acids peptide 265 to 309 presented in Figure 4B to acidic POPG or zwitterionic POPC bicelles (left) as well as to 10% acidic PtdIns(4,5)P2/90% zwitterionic POPC bicelles at different lipid concentrations. One representative of 3 independent experiments is shown. (D) An indirect FRET strategy was used to analyze the proximity between the fluorescent plasma membrane DiO′ probe and p–IL-7Rα$^{Y449}$ located at the carboxyterminal end of the IL-7Rα cytoplasmic domain in bone marrow B220$^{+}$CD43$^{+}$ sorted cells from control (WT, red columns) and VAV-CRE (blue columns) mice, before and after the addition of IL-7 (2 ng/mL) for 2 minutes at 37°C. Representative confocal pictures (original magnification ×63) of energy transfer (FRET efficiency) between AF488 (DIO′)– and AF546 (p–IL-7Rα$^{Y449}$)–labeled secondary antibody. FRET efficiency was calculated according to the indirect FRET method validated by Guala et al (left).[23] The rainbow scale represents the energy transfer between the 2 fluorophores from 0.5 (blue) to 2 (white). The quantitative energy transfer between the 2 fluorophores-labeled DiO′ and p–IL-7Rα$^{Y449}$ (FRET efficiency) is presented (right). Results represent means ± SEM (n = 135-206 cells analyzed per group, from 6 mice). *P* values were calculated using unpaired nonparametric *t* test. NS: $P > .05$; *$P < .05$; **$P < .01$; ***$P < .001$; ****$P < .0001$. NS, nonsignificant; POPC, 1-palmitoyl-2-oleoyl-sn-glycero-3-phosphatidylcholine; POPG, 1-palmitoyl-2-oleoyl-sn-glycero-3-phosphatidylglycerol; SEM, standard error of the mean; WT, wild type; MFI, mean fluorescence intensity; FRET, fluorescence resonance energy transfer.

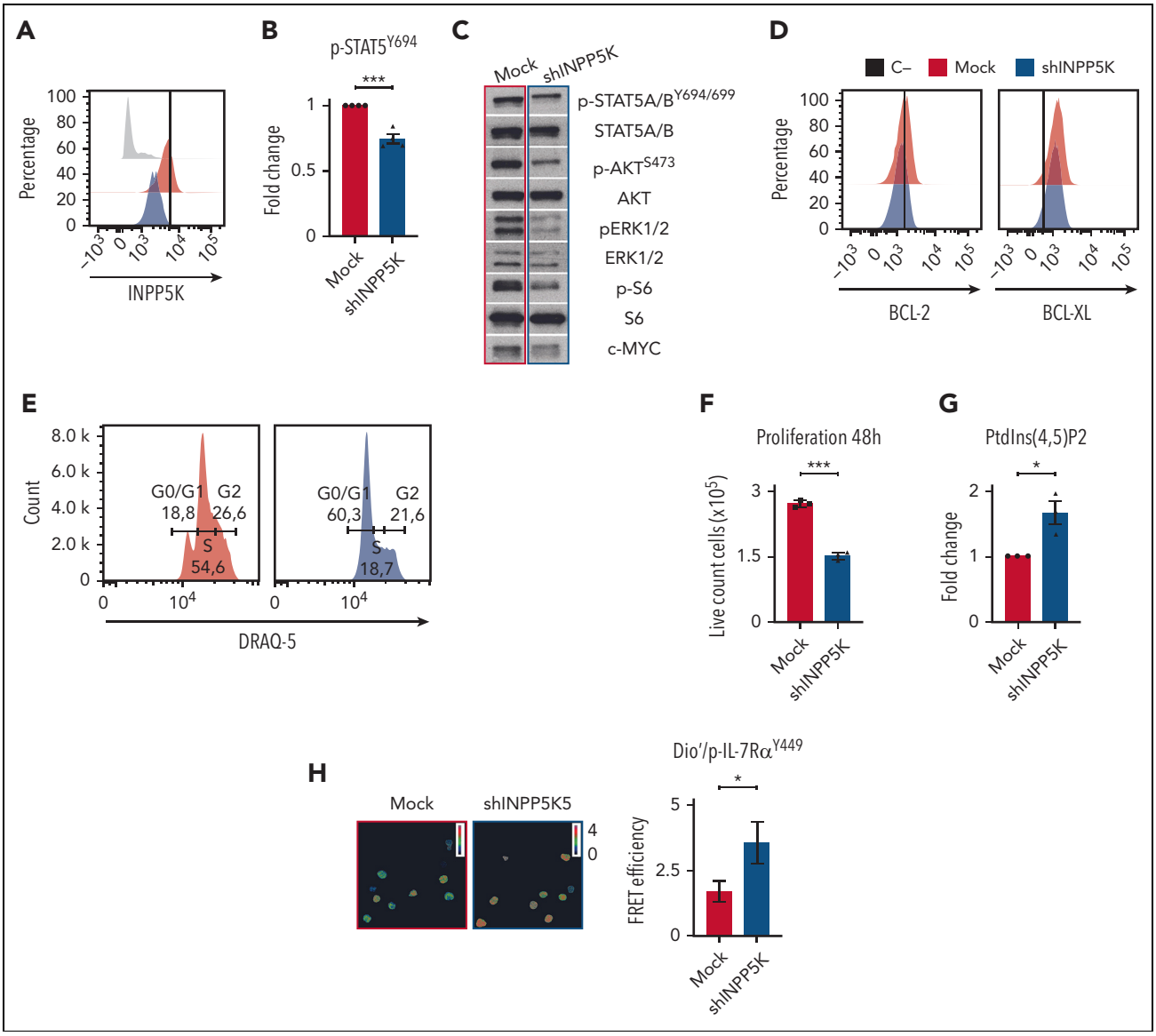


**Figure 4. INPP5K knockdown alters the structure and reduces signaling and cell proliferation of a human mutant CA oncogenic IL-7Rα chain expressed in BaF3 cells.** (A-B) INPP5K (A) and p-STAT5$^{Y694}$ (B) signals were analyzed using flow cytometry in plasma membrane–permeabilized CA–IL-7Rα BaF3 cells transduced with shINPP5K or control mock shRNA (mock). (A) Representative MFI histograms of INPP5K protein signals. C- is the background signal generated by the labeled secondary antibody alone. (B) Quantitative p-STAT5$^{Y694}$ signal after MFI normalization to mock mean MFI. Results represent individual experiments and mean ± SEM. (C) Levels of p-STAT5A/B$^{Y694/699}$, STAT5A/B, p-AKT, AKT, p-S6, S6, p-ERK1/2, ERK1/2, and c-MYC were analyzed by western blotting in mock and shINPP5K CA–IL-7Rα BaF3 cells as described (Almeida et al[6]). (D) BCL-2 and BCL-XL antiapoptotic protein signals were analyzed using flow cytometry in plasma membrane–permeabilized mock and shINPP5K CA–IL-7Rα BaF3 cells. Representative MFI histograms of BCL-2 and BCL-XL protein signals are presented. (E) Cell cycle progression was analyzed using flow cytometry in mock and shINPP5K CA–IL-7Rα BaF3 cells after 15 minutes of incubation with DRAQ-5. The percentage of cells in cycles G0/G1 and G2 is indicated for each condition. (F) Mock and shINPP5K CA–IL-7Rα BaF3 cells were cultured in the absence of growth factors and counted after 48 hours. Results represent mean ± SEM. (G) The PtdIns(4,5)P2 signal was analyzed using flow cytometry in plasma membrane–permeabilized mock and shINPP5K CA–IL-7Rα BaF3 cells. Quantitative PtdIns(4,5)P2 signal after MFI normalization to mock mean MFI. Results represent individual experiments and mean ± SEM. (H) An indirect FRET strategy was used to analyze the proximity between the fluorescent plasma membrane DiO′ probe and p–IL-7Rα$^{Y449}$ located at the carboxyterminal end of the mutant human IL-7Rα cytoplasmic domain in mock and shINPP5K CA–IL-7Rα BaF3 cells. FRET efficiency was calculated per the indirect FRET method validated by Guala et al.[23] The quantitative energy transfer between the 2 fluorophores-labeled DIO′ and p–IL-7Rα$^{Y449}$ (FRET efficiency) is presented. Results represent means ± SD (n = 30-50 cells per group). *P* values were calculated using unpaired nonparametric *t* test. NS: $P > .05$; $^{*}P < .05$; $^{**}P < .01$; $^{***}P < .001$. ERK, extracellular signal-regulated kinase; FRET, fluorescence resonance energy transfer; MFI, mean fluorescence intensity; NS, nonsignificant; SEM, standard error of the mean.

of the signal observed in control shRNA/mock–transduced CA–IL-7Rα BaF3 cells (Figure 4A). Despite this relatively high residual expression of INPP5K protein, basal levels of p-STAT5$^{Y694}$ and p-STAT5A/B$^{Y694/699}$ in CA–IL-7Rα BaF3 cells were significantly decreased upon INPP5K silencing (Figure 4B-C). Similarly, AKT/S6 and ERK1/2 signaling, which are also constitutively activated downstream of mutated IL-7Rα receptors,[6] were downregulated in CA–IL-7Rα BaF3 cells transduced with shINPP5K as compared with that in those transduced with control mock shRNA (Figure 4C). Furthermore, levels of the antiapoptotic BCL-2 and BCL-XL proteins as well as the proto-oncogene c-MYC protein, which are all known to be upregulated by the IL-7R pathway, were downregulated in CA–IL-7Rα BaF3 cells with INPP5K silencing (Figure 4C-D). A similar effect of *Inpp5k* silencing was

detected on cell cycle progression: the percentage of cells in cycle G2 or S was lower in CA–IL-7Rα shINPP5K BaF3 cells than that in CA–IL-7Rα/mock BaF3 cells. Inversely, the percentage of cells in G0/G1 was markedly higher in CA–IL-7Rα shINPP5K BaF3 cells than that in CA–IL-7Rα/mock BaF3 cells (Figure 4E). In agreement, CA–IL-7Rα shINPP5K Ba/F3 cells proliferated less than the mock shRNA–transduced CA–IL-7Rα Ba/F3 control cells (Figure 4F). Mechanistically, the PtdIns(4,5)P2 signal and the energy transfer between the excited donor DiO′ membrane fluorophore and the acceptor fluorophore-labeled antibody bound to p–IL-7Rα$^{Y449}$ were both significantly increased in CA–IL-7Rα BaF3 cells transduced with shINPP5K than in those with control mock shRNA (Figure 4G-H).

Altogether, these results indicate that the knockdown of INPP5K in mouse BaF3 cells stably expressing a human CA–IL-7Rα chain is sufficient to increase PtdIns(4,5)P2 levels, reduce the distance between the polybasic sequence–containing CA–IL-7Rα cytoplasmic domain and the plasma membrane, alter the structure of the mutant IL-7Rα chain, and decrease signaling downstream of this human ALL-associated CA receptor, thus leading to decreased cell proliferation. Because the inactivation of *Inpp5k* specifically in mouse T cells leads to significantly decreased T-cell numbers compared with that in control mice (supplemental Material 5; supplemental Figure 16) and because INPP5K is expressed in human T cells (supplemental Material 5; supplemental Figure 17), the effects of INPP5K knockdown were investigated in the human T-ALL DND-41 cell line carrying the CA p.Leu242_Leu243 insLeuSerArgCys IL-7Rα chain insertion mutation.[25] As for mouse BaF3 cells stably expressing a human CA–IL-7Rα chain, a decreased basal level of p-STAT5$^{Y694}$ and antiapoptotic BCL-2 proteins was observed in DND-41 cells upon INPP5K silencing (supplemental Material 5; supplemental Figure 18).

## Discussion

Using a combination of mouse models of in vivo loss of function of INPP5K in B cells and ex vivo cell biology analyses in primary bone marrow B cells, we discovered a B-cell–intrinsic role for INPP5K in the control of the dynamic structure of IL-7R and its signaling, affecting PAX5 expression and early B-cell development. We show here that the loss of INPP5K is associated with increased levels of PtdIns(4,5)P2 in bone marrow B cells and with altered basal and IL-7–stimulated conformational structure of the IL-7R signaling complex. These structural alterations include the distance between IL-7Rα and γc ectodomains, between JAK1 and JAK3, which are constitutively bound to IL-7Rα and γc cytoplasmic domains, respectively, and between the IL-7Rα cytoplasmic region and the plasma membrane. Our results in B cells lacking INPP5K and in PtdIns(4,5)P2/POPC bicelles suggest that stronger ionic interactions between the very conserved positively charged amino acid sequence in the cytoplasmic IL-7Rα juxtamembrane region and the increased level of negatively charged PtdIns(4,5)P2 play an essential mechanistic role in these structural alterations. Indeed, the IL-7Rα chain and its bound JAK1 kinase seem frozen in a structure which is intermediate between basal and IL-7–stimulated conditions in control B cells. This new pathogenic mechanism linked to reduced INPP5K expression was extended to mutated, homodimeric human IL-7Rα chains, which trigger ALL. Downstream to the wild-type and mutated IL-7 receptors, these dynamic structural alterations are responsible for signaling defects. In mice, these signaling defects result in a significantly decreased expression of EBF1 and PAX5, 2 transcription factors known to be essential for initiating and maintaining B-cell lineage commitment from the fraction A in the bone marrow. In a B-cell line expressing a mutant CA human IL-7Rα chain, these signaling defects result in decreased expressions of anti-apoptotic and proto-oncogenic proteins as well as reduced cell cycle alterations and cell proliferation.

Ionic interactions between polybasic amino acid sequences and plasma membrane acidic phospholipids, including PtdIns(4,5)P2, are known to affect protein subcellular localization, structural conformation, and/or functions.[24] The EGF receptor, the CD3ε and CD3ζ T-cell coreceptors, the membrane immunoglobulin G receptor, and other receptors contain cytoplasmic juxtamembrane polybasic sequences that ionically interact with plasma membrane PIs and through these ionic interactions, control receptor conformation, activity, and downstream signaling.[26-34] In a few cases, reducing the plasma membrane PtdIns(4,5)P2 level via the expressions of exogenous, genetically modified PI 5-phosphatases, such as yeast Inp54p or mammalian INPP5J and synaptojanin, was shown to alter the dynamic conformation of the receptor, affecting its activation and signaling.[29] Our present results extend this pathogenic mechanism to IL-7R and, for the first time to our knowledge, define an endogenous 5-phosphatase that controls plasma membrane PtdIns(4,5)P2 level in this specific context. Thus, we propose a new physiological role for INPP5K that is the control of plasma membrane PtdIns(4,5)P2 in bone marrow B cells, allowing the requisite structure and mobility of the IL-7Rα chain and bound JAK1 kinase for optimal signaling in basal and IL-7–stimulated conditions.

It is noteworthy that the analysis of 35 cytokine receptors in mice and humans for the presence of a positively charged sequence in the first 45 amino acids of the cytoplasmic domain revealed that the IL-7Rα chain, along with the IL-21R chain, which is implicated in immunoglobulin production, has by far the highest isoelectric point and net positive charge at physiological pH in that juxtamembrane region.

The physiological role of the IL-7R signaling pathway is not limited to the control of early B-cell development; this pathway is also critical for T-cell development of both αβ and γδ lineages, for the survival of naïve and memory T cells in the periphery as well as for the development of innate lymphoid cell.[5] Accordingly, the loss of INPP5K in VAV-Cre mice was associated with a decreased number of splenic αβ naïve and memory T cells as well as of lung innate lymphoid cell 2 and γδ T cells, suggesting a similar pathological mechanism involving freezing of the IL-7Rα chain and altered IL-7R signaling in these cells. By contrast, blood concentrations of red cells and platelets, which are not dependent on the IL-7R pathway for their development, were normal in VAV-CRE mice.

The IL-7R signaling pathway is implicated in human and mouse autoimmune and chronic inflammatory diseases as well as in cancer. IL-7R not only favors the survival and proliferation of B- and T-ALL cells but also triggers leukemia development in humans and mice when overactivated or mutated and CA. Our present results indicate that INPP5K is an important regulator of the dynamic structure and signaling of wild-type and mutated leukemia-associated IL-7Rs.

## Acknowledgments

The authors thank the members of the GIGA-Molecular Biology of Diseases Unit for helpful discussions, and Muriel Moser (Institut de Biologie et de Médecine Moléculaires [IBMM], ULB, Gosselies) for help with mice breeding at the IBMM. The authors thank the GIGA-In Vitro Imaging (for cell imaging [Sandra Ormenese, Alexandre Hego, and Gaetan Lefevre] and for flow cytometry [Sandra Ormenese, Raafat Stephan, and Céline Vanwinge]), the GIGA-Viral Vectors & Genome Editing and the GIGA-Mouse Facility platforms at the University of Liège (Liège, Belgium) for reagents, discussions, and technical support.

B.M. and C.-A.V.C. were supported by a grant from the FRIA/FRS-FNRS (Fonds National de la Recherche Scientifique belge, FRIA #2017BM and #2015CAVC, respectively). This work was supported by grants from the Université de Liège (FRS #2016, #2018, and #2020) (S.S.); Actions de Recherche Concertée (ARC) #202125 (S.S.), the Fonds Léon Frédéricq (B.M. and C.-A.V.C.), and the FRS-FNRS (CDR #2018 and PDR #2020) (S.S.).


## Authorship

Contribution: B.M., H.L., J.F., M.D., A.M., and R.M. performed research; B.M., H.L., P.M.-O., C.R., A.R., C.-A.V.C., S.A.S., J.F., M.D., A.A., J.T.B., R.M., C.X., C.J.D., and S.S. designed research and analyzed data; and B.M., H.L., J.T.B., C.X., C.J.D., and S.S. wrote the manuscript.

Conflict-of-interest disclosure: The authors declare no competing financial interests.


The current affiliation for P.M.-O. is BioIVT, Royston, United Kingdom.

The current affiliation for A.R. is Immunology-Vaccinology Laboratory, Department of Infectious and Parasitic Diseases, FARAH, University of Liège, Liège, Belgium.

The current affiliation for S.A.S. is Ablynx Sanofi, Ghent, Belgium.

The current affiliation for A.A. is Laboratory of Lipids and Chronobiology, International Institute of Molecular Mechanisms and Machines, Polish Academy of Sciences, Warsaw, Poland.

ORCID profiles: C.R., 0000-0001-6254-5258; C.-A.V.C., 0000-0001-6283-9029; M.D., 0000-0002-1459-161X; A.M., 0000-0001-7498-9841; A.A., 0000-0003-2429-2100; R.M., 0000-0002-5306-0635; C.J.D., 0000-0002-5723-2449; S.S., 0000-0002-5579-3840.

Correspondence: Stéphane Schurmans, Laboratory of Functional Genetics, GIGA Research Centre, Building B34, Université de Liège, rue de l'Hôpital 11, 4000 Liège, Belgium; email: sschurmans@uliege.be.


## Footnotes


Submitted 20 July 2022; accepted 22 December 2022; prepublished online on *Blood* First Edition 4 January 2023. https://doi.org/10.1182/blood.2022017819.


Data are available on request from the corresponding author, Stéphane Schurmans (sschurmans@uliege.be), or the first author, Bastien Moës (b.moes@uliege.be).

The online version of this article contains a data supplement.

The publication costs of this article were defrayed in part by page charge payment. Therefore, and solely to indicate this fact, this article is hereby marked "advertisement" in accordance with 18 USC section 1734.

## REFERENCES


1. Palmer MJ, Mahajan VS, Trajman LC, et al. Interleukin-7 receptor signaling network: an integrated systems perspective. *Cell Mol Immunol*. 2008;5(2):79-89.
2. Babon JJ, Lucet IS, Murphy JM, Nicola NA, Varghese LN. The molecular regulation of Janus kinase (JAK) activation. *Biochem J*. 2014;462(1):1-13.
3. McElroy CA, Holland PJ, Zhao P, et al. Structural reorganization of the interleukin-7 signaling complex. *Proc Natl Acad Sci U S A*. 2012;109(7):2503-2508.
4. Walsh STR. Structural insights into the common γ-chain family of cytokines and receptors from the interleukin-7 pathway. *Immunol Rev*. 2012;250(1):303-316.
5. Barata JT, Durum SK, Seddon B. Flip the coin: IL-7 and IL-7R in health and disease. *Nat Immunol*. 2019;20(12):1584-1593.
6. Almeida ARM, Neto JL, Cachucho A, et al. Interleukin-7 receptor α mutational activation can initiate precursor B-cell acute lymphoblastic leukemia. *Nat Commun*. 2021;12(1):7268-7283.
7. Shochat C, Tal N, Bandapalli OR, et al. Gain-of-function mutations in interleukin-7 receptor-α (IL7R) in childhood acute lymphoblastic leukemias. *J Exp Med*. 2011;208(5):901-908.
8. Zenatti PP, Ribeiro R, Li W, et al. Oncogenic IL7R gain-of-function mutations in childhood T-cell acute lymphoblastic leukemia. *Nat Genet*. 2011;43(10):932-939.
9. Schurmans S, Vande Catsyne CA, Desmet C, Moës B. The phosphoinositide 5-phosphatase INPP5K: from gene structure to in vivo functions. *Adv Biol Regul*. 2021;79:100760.
10. Pernot E, Terryn S, Cheong SC, et al. The inositol Inpp5k 5-phosphatase affects osmoregulation through the vasopressin-aquaporin 2 pathway in the collecting system. *Pflugers Arch*. 2011;462(6):871-883.
11. Abdelrasoul H, Werner M, Setz CS, et al. PI3K induces B-cell development and regulates B cell identity. *Sci Rep*. 2018;8(1):1327-1341.
12. Clark MR, et al. Orchestrating B cell lymphopoiesis through interplay of IL-7 receptor and pre-B cell receptor signalling. *Nat Rev Immunol*. 2014;14(2):69-80.
13. Hirokawa S, Sato H, Kato I, Kudo K. EBF-regulating Pax5 transcription is enhanced by STAT5 in the early stage of B cells. *Eur J Immunol*. 2003;33(7):1824-1829.
14. Ochiai K, Maienschein-Cline M, Mandal M, et al. A self-reinforcing regulatory network triggered by limiting IL-7 activates pre-BCR signaling and differentiation. *Nat Immunol*. 2012;13(3):300-307.
15. Reth M, Nielsen P. Signaling circuits in early B-cell development. *Adv Immunol*. 2014;122:129-175.
16. Decker T, Pasca di Magliano M, McManus S, et al. Stepwise activation of enhancer and promoter regions of the B cell commitment gene Pax5 in early lymphopoiesis. *Immunity*. 2009;30(4):508-520.
17. Roessler S, Györy I, Imhof S, et al. Distinct promoters mediate the regulation of Ebf1 gene expression by interleukin-7 and Pax5. *Mol Cell Biol*. 2007;27(2):579-594.
18. Corcoran AE, Smart FM, Cowling RJ, Crompton T, Owen MJ, Venkitaraman AR. The interleukin-7 receptor α chain transmits distinct signals for proliferation and differentiation during B lymphopoiesis. *EMBO J*. 1996;15(8):1924-1932.
19. Jiang Q, Li WQ, Hofmeister RR, et al. Distinct regions of the interleukin-7 receptor regulate different Bcl2 family members. *Mol Cell Biol*. 2004;24(14):6501-6513.
20. Lin JX, Migone TS, Tsang M, et al. The role of shared receptor motifs and common Stat proteins in the generation of cytokine pleiotropy and redundancy by IL-2, IL-4, IL-7, IL-13, and IL-15. *Immunity*. 1995;2(4):331-339.
21. Venkitaraman AR, Cowling RJ. Interleukin-7 induces the association of phosphatidylinositol 3-kinase with the alpha chain of the interleukin-7 receptor. *Eur J Immunol*. 1994;24(9):2168-2174.
22. Wofford JA, Wieman HL, Jacobs SR, Zhao Y, Rathmell JC. IL-7 promotes Glut1 trafficking

and glucose uptake via STAT5-mediated activation of Akt to support T-cell survival. *Blood*. 2008;111(4):2101-2111.

23. Guala D, Bernhem K, Ait Blal H, et al. Experimental validation of predicted cancer genes using FRET. *Methods Appl Fluoresc*. 2018;6(3):035007.

24. Li L, Shi X, Guo X, Li H, Xu C. Ionic protein-lipid interaction at the plasma membrane: what can the charge do? *Trends Biochem Sci*. 2014;39(3):130-140.

25. Porcu M, Kleppe M, Gianfelici V, et al. Mutation of the receptor tyrosine phosphatase PTPRC (CD45) in T-cell acute lymphoblastic leukemia. *Blood*. 2012;119(19):4476-4479.

26. Aivazian D, Stern LJ. Phosphorylation of T cell receptor zeta is regulated by a lipid dependent folding transition. *Nat Struct Biol*. 2000;7(11):1023-1026.

27. Arkhipov A, Shan Y, Das R, et al. Architecture and membrane interactions of the EGF receptor. *Cell*. 2013;152(3):557-569.

28. Chen X, Pan W, Sui Y, et al. Acidic phospholipids govern the enhanced activation of IgG-B cell receptor. *Nat Commun*. 2015;6:8552.

29. Chouaki-Benmansour N, Ruminski K, Sartre A-M, et al. Phosphoinositides regulate the TCR/CD3 complex membrane dynamics and activation. *Sci Rep*. 2018;8(1):4966.

30. Deford-Watts LM, Tassin TC, Becker AM, et al. The cytoplasmic tail of the T cell receptor CD3 epsilon subunit contains a phospholipid-binding motif that regulates T cell functions. *J Immunol*. 2009;183(2):1055-1064.

31. Endres NF, Das R, Smith A, et al. Conformational coupling across the plasma membrane in activation of the EGF receptor. *Cell*. 2013;152(3):543-556.

32. Heo WD, Inoue T, Park WS, et al. PI(3,4,5)P3 and PI(4,5)P2 lipids target proteins with polybasic clusters to the plasma membrane. *Science*. 2006;314(5804):1458-1461.

33. Xu C, Gagnon E, Call ME, et al. Regulation of T cell receptor activation by dynamic membrane binding of the CD3ε cytoplasmic tyrosine-based motif. *Cell*. 2008;135(4):702-713.

34. Zhang H, Cordoba S-P, Dushek O, van der Merwe PA. Basic residues in the T-cell receptor ζ cytoplasmic domain mediate membrane association and modulate signaling. *Proc Natl Acad Sci U S A*. 2011;108(48):19323-19328.